 doi:10.20944/preprints201711.0087.v3

Article

Real-life/real-time elderly fall detection with a triaxial accelerometer

A. Sucerquia [1], J.D. López [2,†] and J.F. Vargas-Bonilla [2,‡]

[1] Facultad de Ingenieía, Institución Universitaria ITM, Medellín, Colombia (e-mail luzsucerquia@itm.edu.co)
[2] SISTEMIC, Facultad de Ingeniería, Universidad de Antiquia UDEA, Calle 70 No. 52-21, Tel.: +57-4-2198561, Medellín, Colombia (e-mail †josedavid@udea.edu.co, ‡jesus.vargas@udea.edu.co)
* Correspondence: luzsucerquia@itm.edu.co; Tel.: +57-460-0727 ext. 5586

Abstract: The consequences of a fall on an elderly person can be reduced if the accident is attended by medical personnel within the first hour. Independent elderly people use to stay alone for long periods of time, being in more risk if they suffer a fall. The literature offers several approaches for detecting falls with embedded devices or smartphones using a triaxial accelerometer. Most of these approaches were not tested with the target population, or are not feasible to be implemented in real-life conditions. In this work, we propose a fall detection methodology based on a non-linear classification feature and a Kalman filter with a periodicity detector to reduce the false positive rate. This methodology requires a sampling rate of only 25 Hz; it does not require large computations or memory and it is robust among devices. We test our approach with the SisFall dataset achieving 99.4% of accuracy. Then, we validate it with a new round of simulated activities with young adults and an elderly person. Finally, we give the devices to three elderly persons for full-day validations. They continued with their normal life and the devices behaved as expected.

Keywords: Triaxial accelerometer; Wearable devices; Fall detection; Mobile health-care; SisFall; Kalman filter

1. Introduction

At least one third of elderly people suffers a fall per year and the probability of falling increases with age and previous falls [1–4]. The consequences of a fall can be reduced if the person is attended by medical services within an hour from the accident [5–7]. This timing is feasible with institutionalized elderly people, but healthy independent elderly people use to stay alone for long periods of time increasing their risk of aggravating the injuries in case of an accident. Nowadays, authors focus on developing automatic fall detection systems, which generate an alarm in case of an event, but they still present high error rates in real-life conditions (see [7–10] for reviews on the field). In this paper, we tackle this issue with a novel fall detection methodology tested in real-life situations with the target population, using a simple to implement triaxial-accelerometer-based embedded device.

Detecting falls with a triaxial accelerometer is commonly divided in three stages: pre-processing, feature extraction, and classification. The preprocessing can be as simple as a low-pass filter [11], but it mainly depends on the selected feature extraction. In this sense, there is a wide amount of features available in the literature, such as acceleration peaks, variance, angles, etc. (see [9, Table 4] for a complete list). These features transform the acceleration signal in order to better discriminate between falls and activities of daily living (ADL). Regarding classification, threshold based detection is still the most opted choice over machine learning alternatives, mainly because the latter are impractical for real-time implementation. Habib et al. [10] show various examples of SVM approaches consuming the battery in few hours and Igual et al. [12] concluded that these approaches are highly dependent on the acquisition device used.

A common problem with approaches proposed in the literature is that most of them were tested with young adults under controlled conditions [9, Table 5]. Moreover, previous works demonstrated

 doi:10.20944/preprints201711.0087.v3

that the accuracy of these approaches is significantly reduced when tested on institutionalized [13] and independent [11] elderly people. The main reason authors have for not testing with the target population is the lack of appropriate public datasets and the difficulty of acquiring real falls with elderly people [9,11,13]. In order to tackle these issues, we recently released the SisFall dataset [11], a fall and movement dataset acquired with a triaxial accelerometer mounted on an embedded device attached to the waist (see [14] for implementation details).

In [11], we demonstrated that most failures in fall detection are focused on a few activities. Most of these activities coincide in periodic waveforms (from walk and jog) and high peak acceleration ADL (e.g., jump). There are previous approaches in the literature for detecting jog and walk with accelerometers. Cola et al. [15] detected gait deviation as a fall-risk feature. Oner et al. [16] used the peaks of the acceleration signal measured with a smartphone to detect steps and subsequently the kind of activity based on the period between steps. Wundersitz et al. [17] did it with an embedded device. Other authors used more elaborated metrics but all peak based. Clements et al. [18] computed principal components of the Fast Fourier Transform (FFT), to cite an example. In contrast, we previously developed a more stable gait detector based on wavelet or auto-correlation indistinctly [19]. However, it was too computationally intensive for real-life implementation in an embedded device.

In this work, we present a Kalman-filter-based fall detection algorithm that additionally detects gait as a feature to avoid false positives. The fall detection feature is a novel non-linear metric based on two widely used features: the sum vector magnitude and the standard deviation magnitude. The Kalman filter is a well-known optimal estimator [20] widely used in several research fields. The Kalman filter is Markovian (avoiding large memory storage) and linear (simple computations for lower energy consumption). Here, we use it as an input to the non-linear feature by determining the orientation of the subject: jogging activities may lead to high accelerations, but the absence of inclination implies that the subject is not falling. We additionally use the Kalman filter to smooth gait patterns (as sinusoidal-shape waveforms) in order to feed our gait detector.

The Kalman filter has been previously used to identify movements of interest with accelerometers. Bagalà et al. [21] used it to determine the lie-to-sit-to-stand-to-walk states, which are commonly used to measure the risk of falling in elderly people (with the Berg Balance Scale –BBS– for example [22]). There, the authors used an extended Kalman filter to determine the orientation of the device. Otebolaku et al. [23] proposed a novel user context recognition using a smartphone. In their work, the Kalman filter was used to obtain the orientation of the device based on its multiple sensors (not only the accelerometer). But the authors did not specify how they did it. Finally, Novak et al. [24] used a multiple sensors system to determine gait initiation and termination. In their work, the Kalman filter was used again to obtain the orientation of the device.

Aforementioned works coincide in their objective with the Kalman filter (identifying locomotion activities), but they differ on the way it was implemented and none of them was interested in detecting falls. Some other authors have used the Kalman filter as part of their fall detection algorithms [25–29]. All of them used the triaxial accelerometer together with other sensors (a gyroscope in all cases and a magnetometer in one case). In these works, the Kalman filter was used for de-noising, data fusion, and to obtain the device angle. The main difference among these works is the classification strategy: threshold, SVM, neural networks, or Bayesian classifier.

Our approach differs from these previous works in several key features: (*i*) one of our main purposes is to extend the battery life of the device. Following this, we only use one triaxial accelerometer. We discarded to use a gyroscope because it typically consumes more than ten times more current than the accelerometer ($40 - 145\ \mu$A for the ADXL345 that we selected, compared to hundreds of μA to some mA for a gyroscope). (*ii*) We present a novel non-linear classification feature that allows us to obtain high accuracy values with a simple thresholding approach. (*iii*) We include a gait detector to discard false positives caused by high acceleration periodic activities. (*iv*) We validate on real-time and under uncontrolled conditions with the target population.

Preprints (www.preprints.org) | NOT PEER-REVIEWED | Posted: 6 February 2018 doi:10.20944/preprints201711.0087.v3

This paper continues as follows: In Sections 2 and 3, we present the dataset used and explain the proposed approach. In Section 4, we present the overall results with controlled activities and falls (in simulation and implemented on an embedded device); we perform an individual activity analysis; and we show an on-line validation, where three elderly voluntaries carried an embedded device for several days each. Finally, we discuss our findings in Section 5.

2. Materials

We recently published a dataset with falls and ADL acquired with accelerometer (SisFall: Sistemic research group fall and movement dataset [11]). Here we use this dataset to train and test the proposed approach. It was generated with 38 participants divided in elderly people and young adults. Twenty three young adults performed five repetitions of 19 ADL and 15 fall types, while 14 participants over 62 years old performed 15 ADL. One additional participant, a 60 years old participant, performed both ADL and falls. The dataset was acquired with a self-developed embedded device attached to the waist [14]. The embedded device was based on a Kinets MKL25Z128VLK4 microcontroller with an ADXL345 accelerometer. The accelerometer was configured for $\pm$16 G, 13 bits of ADC, and a sampling rate of 200 Hz.

A second device was developed for validating our methodology (Figure 1). This device consisted of the same microcontroller and sensor used for SisFall, but it included a GPRS transmitter (to send short text messages –SMS) that was activated if a fall was detected. As we did with the first device, it was fixed with a homemade belt (see the supplementary videos of [11]) to guarantee that it did not move relative to the subject. Neither it required to be completely vertical nor to have an additional calibration once the subject wore it.

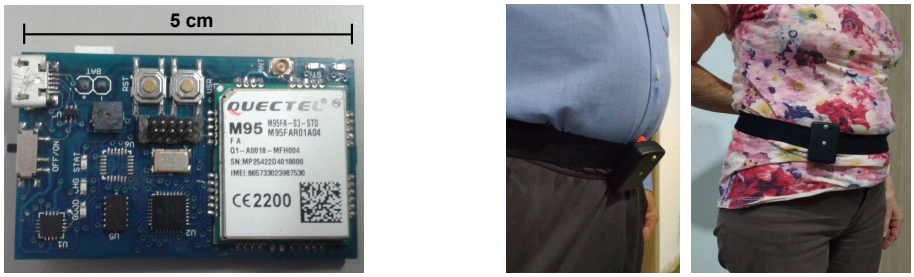

(a) Device used for implementing and testing the proposed approach

(b) Participants using the device

Figure 1. Validation device. (a) With similar characteristics of the device used in [11], this one included a GPRS module able to send text messages in case of alarm. (b) Note how the elderly participants did not wear the device exactly on the expected position/orientation (The photos show positions observed at the end of uncontrolled recordings).

Two additional validation tests were performed with this device:

- Individual activities: Six young adults (subjects SA03, SA04, SA05, SA06, SA09, SA21) and one elderly person (subject SE06) performed again three trials of all activities in SisFall (except D17, getting in and out of a car, due to logistic issues).
- On-line uncontrolled tests: We gave the device to three elderly participants that were not part of SisFall dataset. They were independent and healthy. Table 1 shows their gender, age, height and weight. The subjects used the device permanently for several days, except during sleep and shower (as the device is not water-proof yet). We used three devices to guarantee the integrity of the system.

Preprints (www.preprints.org) | NOT PEER-REVIEWED | Posted: 6 February 2018 doi:10.20944/preprints201711.0087.v3

Table 1. Gender, age, height and weight of the on-line test participants.

Code	Gender	Age	Height [m]	Weight [kg]
SM01	Female	61	1.56	54
SM02	Female	70	1.46	56
SM03	Male	81	1.62	68

All activities performed by the participants were approved by the Bio-ethics Committee of the Medicine Faculty, Universidad de Antioquia UDEA (Medellín, Colombia). Additionally, all participants were evaluated by a sports specialized physician.

3. Methods

Figure 2 shows a schematics of the proposed approach. It includes bias variations of the signal together with acceleration peaks. This increases the robustness of the feature extraction and allows simpler classifiers. The proposed methodology consists of four stages: Preprocessing, feature extraction, classification, and periodic activity detection. For each time sample k, the raw acceleration data $\vec{a}[k]$ is initially low-pass filtered. Then, it splits into bias removal and Kalman filtering, which feeds both features J_1 and J_2 respectively (see Eqs. (8) and (9) below). A threshold-based classification is performed over a non-linear indirect feature. If the resultant value crosses the threshold, the periodicity of the signal (extracted from the Kalman filter and a zero-crossing algorithm) is analyzed in order to determine if it is a false fall alert or if indeed the alarm should be turned on. This methodology is explained in the following section.

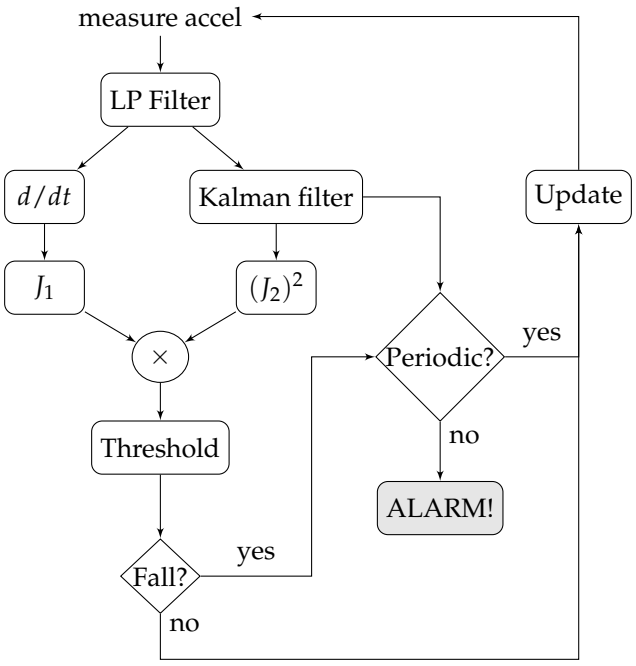

Figure 2. Proposed methodology. It is based on a non-linear feature that allows detecting falls with a simple threshold based detector. Then, false positives are discarded if a periodic activity is detected after the fall.

3.1. Preprocessing and periodicity detector

The same 4-th order IIR low-pass Butterworth filter with a cut-off frequency of 5 Hz proposed in [11] was used in this work. This filter was selected because: (*i*) It can be implemented in simple

Preprints (www.preprints.org) | NOT PEER-REVIEWED | Posted: 6 February 2018 doi:10.20944/preprints201711.0087.v3

embedded devices; (*ii*) It does not require large computations in software; and (*iii*) an increase in the order or in the cut-off frequency does not improve the accuracy; consequently, it does not require higher sampling frequencies. Filtered data are then bias removed with a simple differentiation of consecutive samples, as it is needed to compute the static feature (J_1). SisFall dataset was initially acquired at 200 Hz; however, the proposed methodology only requires 25 Hz to feed the filter. Then, all results presented here correspond to the proper downsampled signals.

The second feature (J_2) is computed over the bias level, which is obtained with a Kalman filter. A Kalman filter [20] is an optimal quadratic estimator able to recover hidden states of a state-space model. It was used here with two purposes: to recover the bias-level variation and to find the periodicity of the signal. To achieve this, the Kalman filter acts as a set of adaptive FIR filters with the objective of estimating parameters/states of a dynamical system. As any Luemberger-type estimator [30], the estimation is improved by working in closed loop, which allows updating the input and using the historic values collected on the Markovian process. Additionally, being a multivariable estimator, the Kalman filter includes both the variance and covariance of the signal to filter (something unfeasible with FIR filters). Finally, as an adaptive filter, it has more immunity to model uncertainty, noise, and perturbations than FIR filters (it is optimal on the quadratic mean, and it is robust).

Let us define the filtered acceleration data as $\vec{a}[k] = [a_x, a_y, a_z]^T \in \Re^{3\times 1}$ for time instant k, where a_x, a_y, and a_z are single samples of raw acceleration (in practice, it comes in bits, as acquired by the ADC of the device). These data feed the following autonomous state-space model:

$$\begin{aligned} \vec{x}[k] &= A\vec{x}[k-1] + \eta \\ \vec{y}[k] &= C\vec{x}[k] + \epsilon \end{aligned} \tag{1}$$

where the first three states of $\vec{x} \in \Re^{4\times 1}$ are used for classification and the fourth state x_4 removes peaks from periodic signals (see Figure 3, example with activity F05: jog, trip, and fall). As this Kalman filter is exclusively used for smoothing (and not for feature extraction or classification), the state transition $A \in \Re^{4\times 4}$ and output $C \in \Re^{4\times 4}$ matrices are identity matrices. Finally, the output is defined as $\vec{y} = [a_x, a_y, a_z, a_y - b_{a_y}]^T \in \Re^{4\times 1}$, where the first three terms are the low-pass filtered acceleration data in the three axis and the fourth output is the acceleration on vertical axis minus its current bias b_{a_y}. The vertical bias $b_{a_y}[k]$ is dynamically updated with a sliding window of 1 s over the mean of the output of the Kalman filter. x_4 provides a zero-bias sinusoidal-shape waveform when the acceleration comes from periodic activities (walk, jog, going-up stairs, etc.). The period of this signal can be detected counting zero-crossings (changes of sing) and dividing by two over a given time window.

This state-space model is affected by Gaussian measurement noise $\epsilon = \mathcal{N}(0, R)$, and Gaussian state uncertainty $\eta = \mathcal{N}(0, Q)$. The objective of the Kalman filter is to minimize the variance of the states $P \in \Re^{4\times 4}$, considering them as random variables with a Gaussian distribution: $\vec{x} = \mathcal{N}(\bar{x}, P)$.

The Kalman filter consists of five equations divided in two stages. The prediction stage of the Kalman filter predicts the current value of the states and their variance solely based on their previous values:

$$\vec{x}[k]^- = A\vec{x}[k-1] \tag{2}$$

$$P[k]^- = AP[k-1]A^T + Q \tag{3}$$

Both $\vec{x}[k]^-$ and $P[k]^-$ are intermediate values that must be corrected based on current data values:

Preprints (www.preprints.org) | NOT PEER-REVIEWED | Posted: 6 February 2018 doi:10.20944/preprints201711.0087.v3

$$G[k] = CP[k](CP[k]^{-}C^{T} + R)^{-1} \quad (4)$$

$$\vec{x}[k] = \vec{x}[k]^{-} + G[k](\vec{y}[k] - C\vec{x}[k]^{-}) \quad (5)$$

$$P[k] = (I_4 - G[k]^{T}C)P[k]^{-} \quad (6)$$

where $I_4 \in \Re^{4\times4}$ is a (4×4) identity matrix.

This strategy only requires to sintonize two parameters to set-up the Kalman filter: the variance matrices Q and R. There are not rules to determine their values, but specifically for this problem they are not difficult to define. Both are usually diagonal (no interaction among states), large values of Q and R tend to the original data: $\vec{x} \approx \vec{y}$, and they are also complementary, i.e., the states are flatten when reducing any of them. As shown in Figure 3 (Second and Third panels), the first three states are flat (inclination of the subject) and the fourth one seeks for periodic (sinusoidal shape) waveforms.

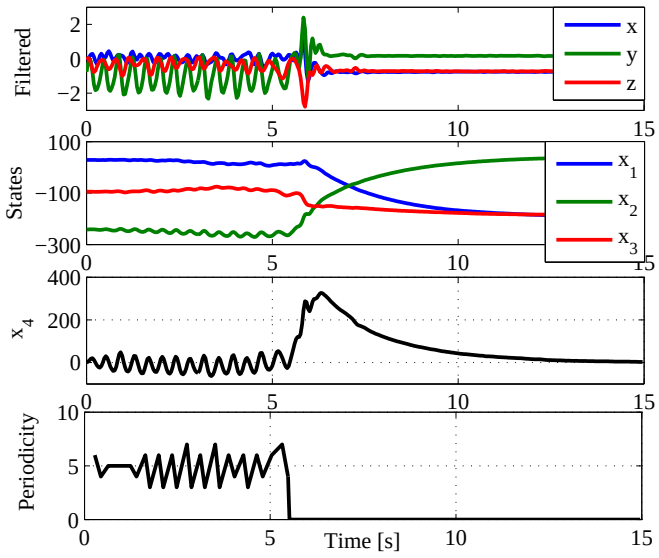

Figure 3. Kalman filtering.(Top panel) Reference filtered acceleration data (Activity F05 of SisFall: jog, trip, and fall) in gravities [G]. (Second panel) First three states of the Kalman filter. The filter estimates the bias-level variations of the signal. (Third panel) The forth state of the Kalman filter recovers a quasi sinusoidal signal during the first 6 s. Its objective is to dynamically remove bias to allow posterior zero crossing detection. (Bottom panel) Periodicity detector. The first 6 s the subject is jogging with a period of 10 time samples (half zero crossings); when the subject suffers a fall it stops detecting periodicity too.

The states can be initialized with zero values, and $P[0] = Q$, i.e., selecting uninformative priors. However, for faster convergence $x_2[0]$ and $b_{a_y}[0]$ can be initialized with -1 G (approx. -258 in bytes for the device configuration used here), which is the initial condition of the accelerometer in our device. Q and R can be computed with a simple heuristic process: Using a walk and fall file for testing, (*i*) Initialize Q and R with identity matrices; then, (*ii*) for the first three states (first three diagonal values of Q and R) start an iterative process by reducing by 10 the standard deviation (square of each diagonal value) of Q and then doing the same with R, until the states start looking flat. A good fit can be done by reducing the scale to 5 and then to 2; although these matrices are poorly sensitive, i.e., the algorithm can work with approximate values. Finally, (*iii*) for the fourth state reduce Q and R (as in the previous step) until x_4 shows a sinusoidal shape in periodic activities (walk and jog). The objective is to clean peaks near zero. Preliminary tests (not shown here) demonstrated that the accuracy is not affected by small variations on these parameters. The final values used in this work were:

Preprints (www.preprints.org) | NOT PEER-REVIEWED | Posted: 6 February 2018 doi:10.20944/preprints201711.0087.v3

$$Q = 0.001^2 \times I_4 \qquad R = \begin{bmatrix} 0.05^2 & 0 & 0 & 0 \\ 0 & 0.05^2 & 0 & 0 \\ 0 & 0 & 0.05^2 & 0 \\ 0 & 0 & 0 & 0.01^2 \end{bmatrix} \tag{7}$$

These values are approximated to those obtained by He et al., [27] for setting-up their Kalman filter. They applied an auto-regressive model to determine A (their final value was almost an identity matrix), Q, and R. In practice, all computations in both the computer (Matlab, Mathworks) and the embedded device are performed in bits and not in gravities to reduce the computational burden.

Figure 3 (Bottom panel) shows how state x_4 tends to a zero-bias sinusoidal shape when the person walks or jogs. This allows implementing a simple zero-crossing periodicity detector. Note how the periodicity is lost when the person trips and falls. The periodicity detector analyzes three seconds after a possible fall event. If during this 3 s window the periodicity is kept stable, we may expect that it was not a fall. The size of the window is selected as the minimum to guarantee that the person is slowly walking.

3.2. Feature extraction and classification

The feature extraction consists of a non-linear feature composed of two widely used ones, the sum vector magnitude and the standard deviation magnitude. The static sum vector magnitude is computed as the root-mean-square (RMS) of the static acceleration with previous bias removal:

$$J_1[k] = \text{RMS}(\vec{a}[k] - \vec{a}[k-1]) \tag{8}$$

where the bias is rejected with differentiation.

The standard deviation magnitude is computed at each time step k over a 1 s sliding window of the first three states of the Kalman filter: $\tilde{x}[k] = [\vec{x}[k-N], \ldots, \vec{x}[k]] \in \Re^{3\times N}$, where $N = 25$ is the size of the window (for a frequency sample of 25 Hz). This second feature is computed as follows:

$$J_2[k] = \text{RMS}(\text{std}(\tilde{x}[k])) \tag{9}$$

where $\text{std}(\cdot)$ is the standard deviation operator. The size of the window is selected as the one that includes the three stages of the fall: the pre-fall, the hit, and the time just after it [31]. Testing with windows between 0.25 and 2 s did not improve the accuracy, as expected [11].

The same sliding window can be used to determine the current bias on the y axis: $b_{a_y}[k] = \text{mean}(\tilde{x}_y[k])$. Figure 4 shows both features with the jog-trip-fall example of Figure 3. The maximum values during jogging are half way of the fall in J_1, but they get clearly distant in J_2.

Preprints (www.preprints.org) | NOT PEER-REVIEWED | Posted: 6 February 2018 doi:10.20944/preprints201711.0087.v3

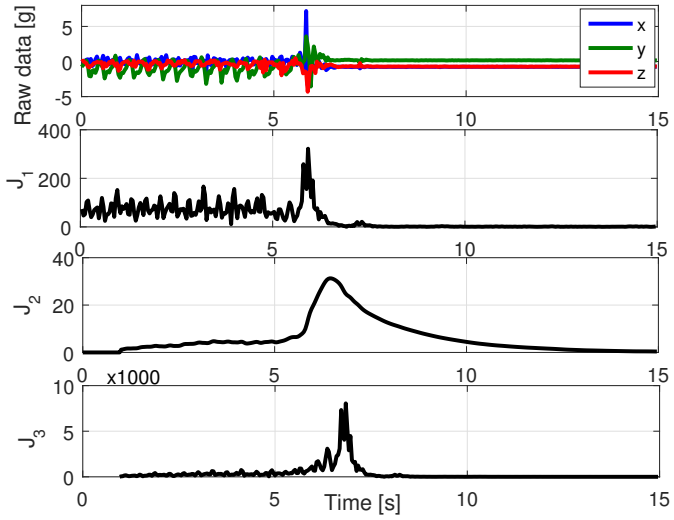

Figure 4. Feature extraction. (Top panel) Reference raw data (The subject is running, trips and falls). (Second panel) Feature J_1 detects the fall as a large difference between its peak and jogging peaks. (Third panel) Feature J_2 has a similar shape but with a larger percentual difference. Both J_1 and J_2 are computed in bits for reducing computations on the embedded device. (Bottom panel) J_3 is formed by J_1 and J_2, increasing their coincidences and diminishing their differences.

Finally, the classification stage is performed over an indirect feature:

$$J_3[k] = \max(\tilde{J}_1[k]) \cdot \max(\tilde{J}_2[k])^2 \tag{10}$$

With $\tilde{J}_i[k] \in \Re^{N\times 1}$ a sliding window with the last N values of the corresponding feature. This window is necessary as the Kalman filter takes some time to achieve the maximum, i.e., not always both metrics present a maximum at the same time. The objective of this product of features is to amplify the values of those activities where both features agree and to minimize those where both features disagree (see Figure 4, bottom panel). The square of J_2 prioritizes it over J_1, as it is more accurate [11].

The classification consists of a single threshold over $J_3[k]$ computed at each time step k. The value of the threshold is defined after a training process. The robustness of the threshold was analyzed with a cross-validation set-up. This analysis was performed guaranteeing the same proportion of falls and ADL in all groups (4510 files randomly divided in 10 groups). A 10-fold cross-validation was performed, each fold had 4059 files for training and 451 for validation. Each group was used in one round as validation data.

Considering that most falls used for training come from young adults, we have taken in consideration two facts observed in [11]: (*i*) The elderly adults show in average lower accelerations in both ADL and falls (this behavior was originally studied in [32]); and (*ii*) the elderly adult that simulated falls always tried harder than the young adults to avoid hitting when falling, which is what one would expect from someone having an accident. These two facts turn into one recommendation: if there is a range for selecting the threshold, the lower acceleration value should be selected to avoid false negatives.

Accuracy (ACC), Sensitivity (SEN), and specificity (SPE) were used as performance metrics. SEN and SPE were calculated as specified in [33]:

$$\text{SEN} = \frac{TP}{TP + FN} \qquad \text{SPE} = \frac{TN}{TN + FP} \tag{11}$$

Preprints (www.preprints.org) | NOT PEER-REVIEWED | Posted: 6 February 2018 doi:10.20944/preprints201711.0087.v3

where TP is the number of falls correctly classified, FN accounts falls that the algorithm did not detect, TN numbers ADL correctly classified, and FP indicates false falls. The accuracy was calculated using Eq. (12):

$$\mathrm{ACC} = \frac{\mathrm{SEN} + \mathrm{SPE}}{2} \tag{12}$$

This balanced computation of the accuracy is selected due to the large difference between the number of ADL and fall files.

3.3. Power consumption

This methodology presents several advantages in terms of power efficiency:

- **Sampling frequency:** Working directly with the inclination of the subject and not with the peak of the fall allows reducing the sampling frequency from the usual 50–100 Hz to just 25 Hz. Considering that the fall detection algorithm must be computed every time that a new sample arrives, this translates in computing it half the times than other works usually do. In terms of power consumption, this means that the device will be at idle state for longer time windows, with the consequent reduction on battery consumption.
- **Number of sensors:** There is a large difference in power consumption between an accelerometer and a gyroscope (with wide variations depending on references, but with the same trend). The gyroscope consumes in average between six and ten times more current than an accelerometer (hundreds of μA compared to tens of μA). Assuming that the fall detection algorithm consumes similar current with or without a gyroscope, we can estimate the reduction on the battery charge in the same scale; i.e., a device without a gyroscope (like ours) could stay active for five to ten times longer than one with it.
- **Threshold based classifier:** In recent years, authors have focused on machine-learning-based classifiers. The reason is clear, there is already a large amount of features (see [9, Table 4]), but none of them has proven to be discriminant enough. By non-linearly combining well-known metrics, we have powered our discrimination feature. Our approach, although simple, allowed us to go back to a simple threshold classifier, which significantly reduces the power consumption compared for example to support vector machines [9].

4. Results

4.1. Fall detection

We initially tested the performance of the proposed algorithm without detecting periodic activities. Table 2 shows the validation results with SisFall dataset over a 10-fold cross-validation (451 files each). All subjects and activities available in the dataset were included in the cross validation. The low detection accuracy obtained with J_1 (around 86 %) would raise questions about its usefulness. However, note how J_3 is significantly higher than J_2 (99.3 % vs. 96.5 %), i.e., although J_1 is not a good metric, combined with J_2, it improves the individual accuracy values.

Table 2. Test on SisFall dataset without periodicity detector.

	J_1	J_2	J_3
Sensitivity [%]	92.92 ±1.56	96.06 ±1.52	99.27 ±0.78
Specificity [%]	81.72 ±2.22	96.79 ±1.12	99.37 ±0.36
Accuracy [%]	86.14 ±1.36	96.50 ±0.84	99.33 ±0.28
Threshold	110.88 ±3.23	22.88 ±0.027	42628 ±511.59

Figure 5 shows an activity-by-activity analysis for the three metrics. The horizontal red line is the threshold for the best accuracy value and the vertical red line divides ADL and falls. By comparing J_1

Preprints (www.preprints.org) | NOT PEER-REVIEWED | Posted: 6 February 2018 doi:10.20944/preprints201711.0087.v3

(Figure 5(a)) and J_2 (Figure 5(b)), we observe that J_1 largely fails in periodic ADL (D03, D04, D06, D18, and D19) while J_2 does not, and J_2 goes closer to the threshold in activities where J_1 does not (D16 for example). This separation was the basis to create J_3; it combines their results with a product but giving priority to J_2 (computed with square), given that it is more accurate. The small box in Figure 5(c) shows how all activities are more separated from the threshold and, more important, less fall files crossed the threshold (false negatives). This initial result significantly improves those obtained with previous approaches tested in [11] (none of them achieved more than 96 %).

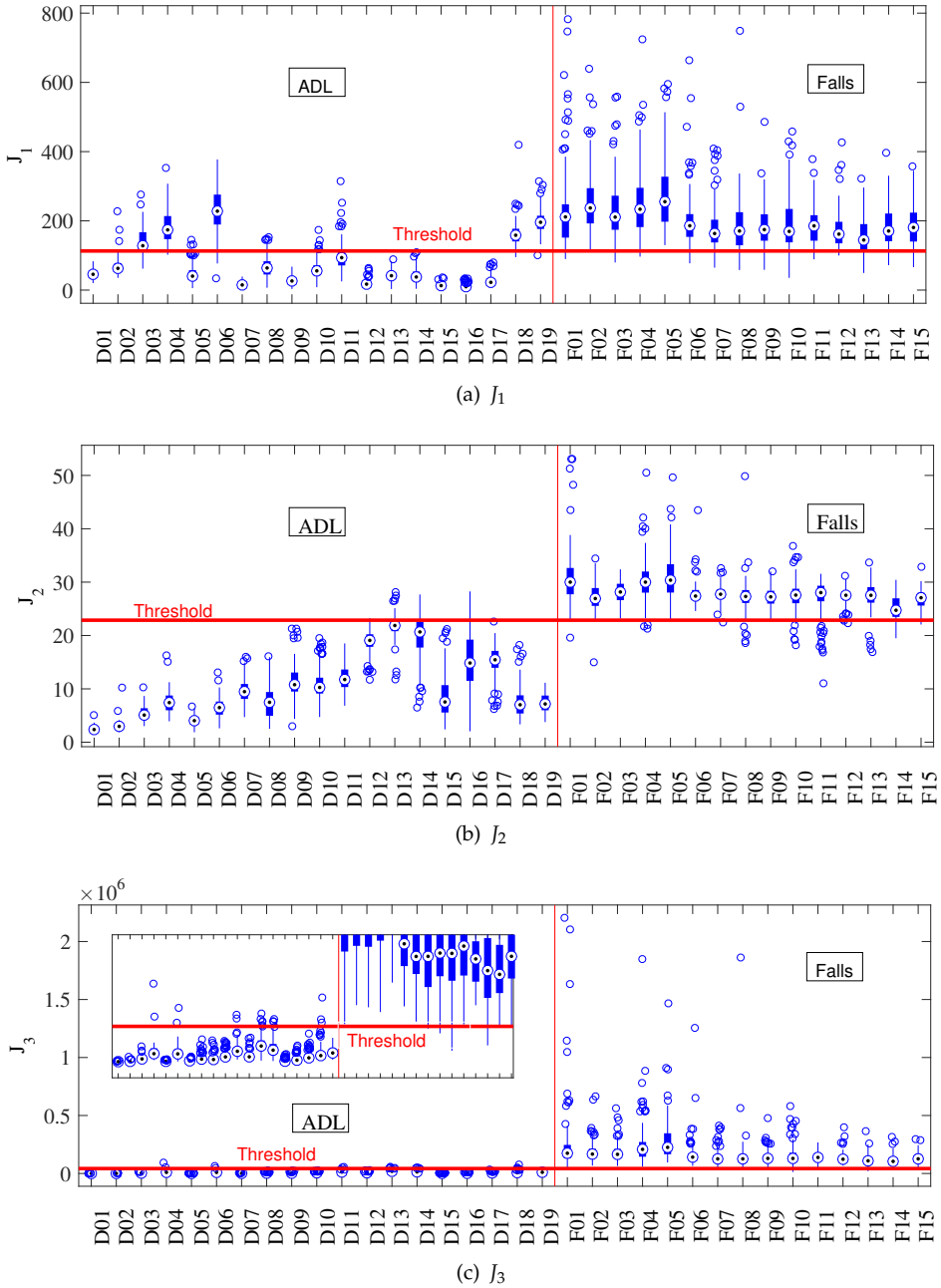

(a) J_1

(b) J_2

(c) J_3

Figure 5. Individual activity analysis of the proposed algorithm tested with SisFall. The horizontal red line corresponds to the optimal threshold value, and the vertical one separates ADL and falls. (a) J_1 has large errors on periodic activities, while (b) J_2 fails in those that change the body angle. (c) They provide to J_3 a better discriminant capability (the small box at the left shows a vertical zoom).

Preprints (www.preprints.org) | NOT PEER-REVIEWED | Posted: 6 February 2018 doi:10.20944/preprints201711.0087.v3

We performed an additional test without including the Kalman filter in order to determine its effect on the algorithm. As expected, the accuracy of all metrics was significantly reduced: 82.65 % for J_1, 91.03 % for J_2, and 83.73 % for J_3. However, this is not a fair comparison. The Kalman filter could be replaced by a set of band-pass filters and similar results should be obtained. But this strategy could severely affect the computational effort of the embedded device and its battery consumption.

4.2. Fall detection with periodicity detector

We then performed the same analysis but including the periodicity detector. The main purpose of this detector is to take J_1 to zero if a periodic activity is observed after a possible fall (false positive) –Same result is obtained if J_2 is selected. Table 3 shows the validation results after a 10-fold cross-validation. Compared to the previous analysis, J_1 has 8 % of improvement (94.32 %). Although one would expect a similar improvement in J_3, this is not the case (although it is higher, with 99.4 % of accuracy) provided that on SisFall dataset, walk and jog only have one file per subject. Nevertheless, the periodicity detector was active in 606 files (13.5 % of the dataset).

Every dataset has a limited number of repetitions per activity. SisFall for example contains only one 1 minute repetition of walk per subject. However, it is expected that a walk will last more than one minute, i.e., the possibility of failure is higher with activities that the subject performs regularly (such as walking). Additionally, Figure 6 shows how the possibility of errors in other activities is lower due to their larger distance from the threshold.

Table 3. Test on SisFall dataset with periodicity detector.

	J_1	J_2	J_3
Sensitivity [%]	97.35 ±1.37	96.15 ±1.59	99.28 ±0.59
Specificity [%]	91.49 ±1.74	96.69 ±1.30	99.51 ±0.48
Accuracy [%]	94.42 ±1.33	96.42 ±0.58	99.39 ±0.36
Threshold	103.03 ±0.02	22.914 ±0.11	42230 ±985.01

Figure 6 shows the same individual activity analysis of Figure 5 but with the periodicity detector in J_1. Figure 6 shows how activities D01 to D04 were turned to zero, as the detector confirmed that the subject was walking or jogging. In this case, J_3 shows more distance from the threshold than on the previous test (the threshold is updated accordingly). This indicates that even the cross-validation did not show a significant improvement on accuracy, the inclusion of the periodicity detector increased the robustness of the algorithm. Importantly, none fall was turned to zero in Figure 6, indicating that the periodicity detector was turned off in all periodic activities that finished in a fall.

Preprints (www.preprints.org) | NOT PEER-REVIEWED | Posted: 6 February 2018 doi:10.20944/preprints201711.0087.v3

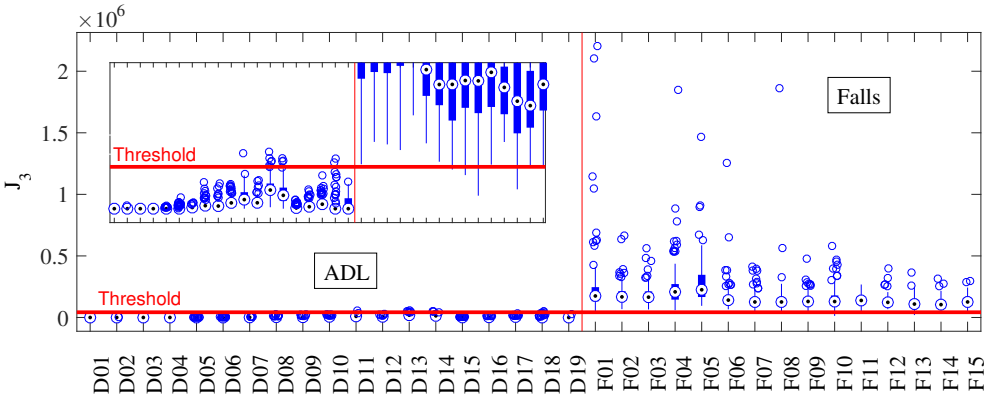

Figure 6. Individual activity analysis of the proposed algorithm including the periodicity detector. The horizontal red line corresponds to the optimal threshold value, and the vertical red line separates ADL and falls. J_3 was turned to zero in all periodic ADL, this allowed it to increase the distance between most ADL and Falls.

4.3. On-line validation

In order to verify the off-line results presented in Table 3, we repeated the activities of SisFall with six young adults and an elderly person with the algorithm implemented on the device (see Section 2). During the tests, we verified on-line if the alarm was turned on (with an indicator incorporated to the device). Additionally, all raw data and the device computations were recorded in text files. We obtained no significant differences between the device and the computer. The proposed approach was implemented on the embedded device with the same parameters and sample frequency defined above (25 Hz). The threshold for J_3 was set at 40,000. The six volunteers performed 18 types of ADL and 15 types of fall in the same way that SisFall dataset was acquired (around 100 total trials per subject).

The participants presented a total of 4 false positives and 1 false negative. Subject SE06 (the elderly person) did not show errors. All false positives were in D13 and D14 (bed related ones). Following Figure 6, it is clear that these activities are commonly close to the threshold. A deeper analysis of this problem (which is not reflected in the following test) demonstrated that when a person moves on the bed, it is usual to separate the hip from the mattress and let it fall in the new position. The pad used for this experiment is harder than a mattress increasing the false positive probability. The overall results coincided with the statistics expected from Table 3.

4.4. Full-day (pilot) tests

We invited three independent elderly participants that were not part of SisFall acquisition (in order to avoid biases) to carry the device for full days (see Section 2). We asked them to behave normally while carrying the device during the day, and we checked the integrity of the devices every couple of hours. They used the device permanently except during night sleep and shower. The files were cut in segments to avoid computational overloads (one hour of recording implied a text file of approx. 10 MB). This is a summary of the recorded activities:

- SM01: She assisted to Tae-Bo dancing lessons for adults (INDER Medellín, Colombia), and stayed at home cooking, washing clothes, cleaning, and resting. She also made several trips to downtown, walked on the street, and traveled by motorcycle.
- SM02: She stayed most of the time cooking at home, cleaning, and sitting on the dining room. She is a dressmaker, so she stays long periods sit at home. She also made some trips by bus; and the last two days she was sick resting at home.
- SM03: He did some trips to a business downtown and to a church. The rest of the time, he stayed at home on bed or in the dining room (reading). In Figure 7 we show one of his trips downtown

Preprints (www.preprints.org) | NOT PEER-REVIEWED | Posted: 6 February 2018 doi:10.20944/preprints201711.0087.v3

(file SM03_1 of [34]). This trip included stairs, two train trips, and two bus trips. Note that despite the wide amount of activities, the levels of feature J_3 were not close to the threshold (40,000).

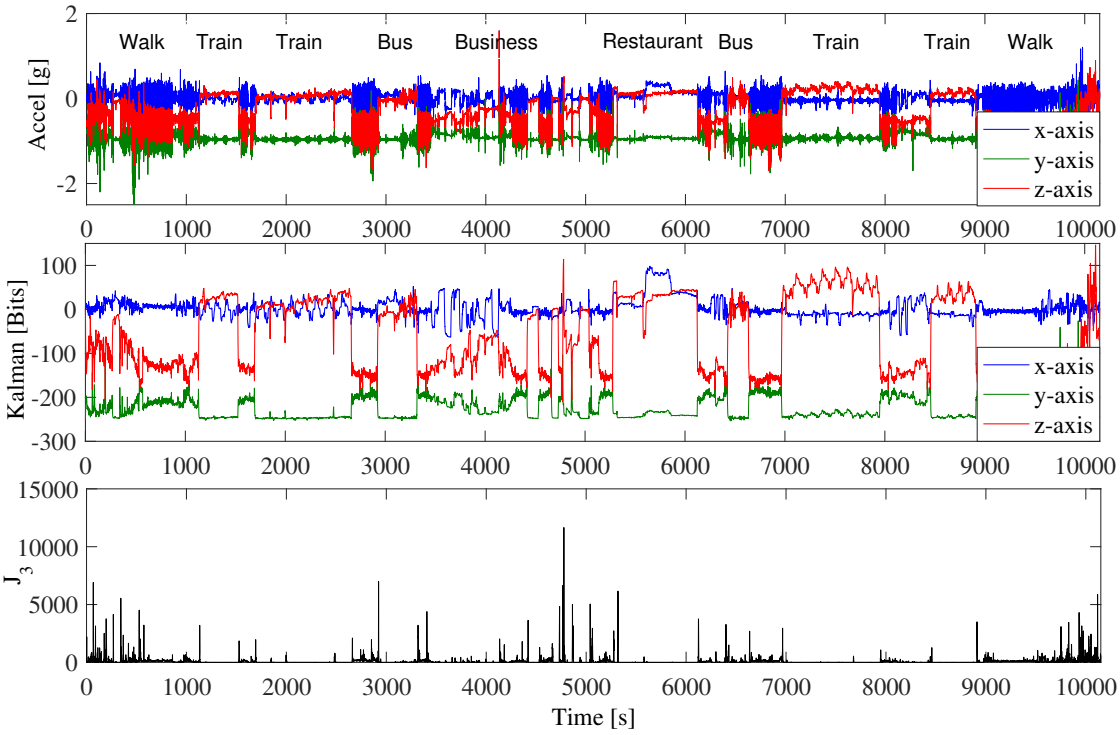

Figure 7. Trip to the downtown of subject SM03. (Top panel) Raw acceleration data, 2 hours and 45 minutes of recording. (Second panel) First three states of the Kalman filter. (Third panel) feature J_3. It was always below the threshold (set at 40,000). Data recorded and processed with the embedded device of Figure 1.

We recorded approx. 170 hours of uncontrolled ADL divided in 77 text files. This dataset is available for download [34]. It includes raw acceleration data, low-pass filtered data, the states of the Kalman filter, the three classification features (J_1, J_2, and J_3), and an indicator of falls detected. These data were recorded with three embedded devices. We additionally released a binnacle of the activities performed by the participants and our explanation for every false positive.

The behavior of our devices is presented as follows:

- SM01: She had nine false positives during the recordings. Four of them were generated when standing up from a low chair or from the sidewalk. As shown in Figure 8(a), she used to stand up fast and her acceleration was close to the threshold. Another two false positives were generated when going downstairs (see Figure 8(b)). And the final three false positives were undetermined (presumably by direct hits to the device).

  The subject is an active person and overall, her movements showed accelerations close (and sometimes higher) to young adults. This behavior contradicts findings of [32]. Our finding suggest that independent elderly people may show the same accelerations for ADL than young adults. Consequently, simulating with young people could be more feasible to compare with uncontrolled ADL of elderly people than simulating ADL with elderly people, who always showed lower acceleration values.

Preprints (www.preprints.org) | NOT PEER-REVIEWED | Posted: 6 February 2018 doi:10.20944/preprints201711.0087.v3

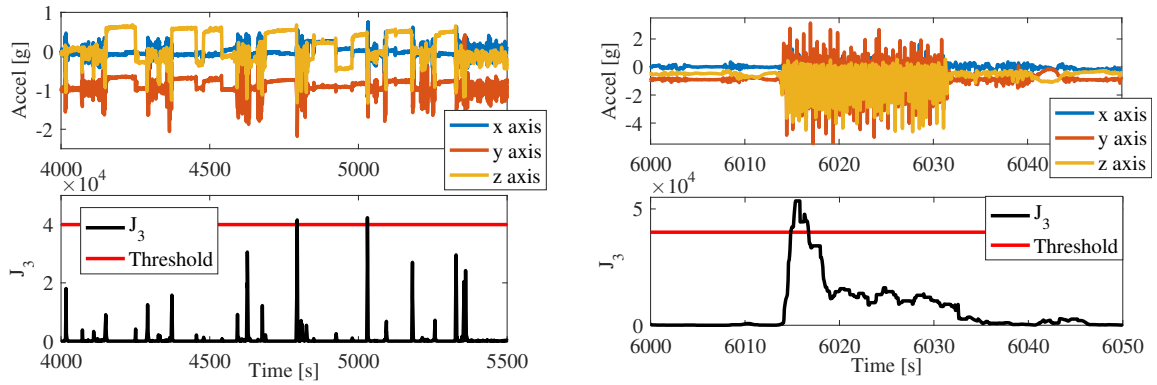

(a) When standing up from a low chair (b) When going downstairs

Figure 8. False positives. Subject SM01 showed high accelerations for everyday activities. (a) Note that her accelerations when standing up from a low chair just crossed the threshold. (b) The periodicity detector did not work correctly when going downstairs because the subject suddenly started the activity and the Kalman filter requires a few steps to compute the period.

- SM02: She had a total of seven false positives. One was a false positive for sitting fast on a chair. Other five false positives were generated because she usually supported her belly against the kitchen or the table. She went out of her home several times, unfortunately in two of them the device got hits and lost the SD card. This is worrying as after an interview, we concluded that she strongly hit the device in both cases presumably against furniture. We presume that it was caused by her low height and by the shape of her belly (See Figure 1(b)). In order to solve this issue, we asked her to use the device on the inner side of the belt (i.e., z-axis pointing towards the back of the subject). After this modification she did not have more false positives.
- SM03: The subject did not have false positives.

In total, there were 16 false positives on this validation test (divided in two subjects). It is interesting that the number of false positives goes down with age. Indeed, when we changed the direction of the device of SM02, she did not present more false alarms. If we consider all falls, this means approximately one false alarm every 10 hours. This is a high value, but it would be reduced with some adjustments: (*i*) As shown in Figure 8(a), we could slightly increase the threshold after some training for highly active elderly subjects. (*ii*) Once we put the device of SM02 on the inner side of the belt, she stopped hitting it against furniture. She also used the device slightly to the right, we cannot determine the effect on the performance in case of a fall, but the data does not show significant differences on ADL. (*iii*) None of the subjects presented false positives during trips (even when traveling by motorcycle). We consider that this is a good measure of performance. Finally, false alarms at the very beginning or ending of the files were not considered for analysis. They were caused by devices turned on a direction different to vertical, or by taking the device off the belt before turning it off.

5. Discussion and Conclusions

In this paper, we presented a fall detection methodology with the following features: Simple frequency filtering, a non-linear feature based on commonly used ones, threshold-based classification, and a periodicity detector to avoid false positives. With these features, we generated a novel fall detection algorithm centered on a Kalman filter stage and a non-linear classification feature. The Kalman filter is not computationally intensive as it is Markovian and it demonstrated to be stable with acceleration data. We selected the Kalman filter because of its low computational cost and robustness; it provided an orientation level to a variance feature and at the same time a sinusoidal signal when the subject performed a periodic activity. This last result highly reduced the computational cost to

 doi:10.20944/preprints201711.0087.v3

obtain the period of the signal, as it avoids to compute more elaborated approaches such as Wavelets or auto-correlation [19].

The most significant improvement of this approach is the way how a combined non-linear feature (J_3) provided higher accuracy (99.4 % with SisFall dataset) than the individual features (94.3 % and 96.4 %, respectively). We obtained this feature after analyzing individually several features with each activity (finally keeping J_1 and J_2). They were selected as they were highly complementary (each fails in different activities). The new non-linear feature used for this work was obtained in an intuitive way and together with a threshold based classifier achieved 99.4 % of accuracy with SisFall dataset.

We implemented this methodology in embedded devices and tested it by redoing on-line all SisFall activities. Then, we validated our work with full-day tests with the target population (two female and one male, all over 60 years old). We asked them to do what they used to do, including traveling by train and bus, doing exercise and cooking or cleaning. The devices behaved as expected; with some false positives due to going downstairs, standing up from a low chair, and by direct hits to the device. This final cause of false positives is out of the scope of this work and a good starting point for a future analysis.

This final validation demonstrated that the proposed methodology can be used in real-life with target population. We recorded and released [34] more than 170 hours of ADL recording with the target population under uncontrolled conditions. This is to our knowledge the largest validation dataset used for a fall detection approach. However, only real falls that may occur at any moment will show the real accuracy of our approach.

This extensive validation additionally allowed us to observe how the devices behaved in terms of power consumption. In average, one battery charge lasted between four and five days (with the device turned off when the subjects were night sleeping) under commercial use configuration (i.e., without recording data). We point out that this result is not conclusive or subject to comparison because it mostly depends on the battery characteristics and hardware configuration, and none of these data are usually released by authors. However, this result demonstrates that our device accomplishes with the full-day single-charge requirement for being feasible under real-life use. Moreover, we consider that our approach is energy efficient because: (*i*) Sampling at 25 Hz instead of the usual 50–100 Hz implies to be active for less time. (*ii*) With respect to the number of sensors, the gyroscope for example consumes several times the current of the accelerometer (hundreds of μA compared to tens of μA), i.e. having only one triaxial accelerometer avoids extra consumption. Finally, (*iii*) the Kalman filter is not computationally intensive, and using a threshold based classification is optimal in terms of computing load. Compared with neural networks or support vector machines, our approach is significantly more efficient [9].

Acknowledgments: This work was supported by project: "Plataforma tecnológica para los servicios de teleasistencia, emergencias médicas, seguimiento y monitoreo permanente a los pacientes y apoyo a los programas de promoción y prevención", code "Ruta-N: FP44842-512C-2013". A. Sucerquia thanks Instituto Tecnologico Metropolitano –ITM for their support on this work.

Author Contributions: All authors conceived and designed the approach; A.S. performed the experiments; A.S. and J.D.L. analyzed the results; and all authors read and approved the final manuscript.

Conflicts of Interest: The authors declare no conflict of interest.

1. Masdeu, J.; Sudarsky, L.; Wolfson, L. *Gait Disorders of Aging. Falls and Therapeutic Strategies.*; Lippincot -Raven, Philadelphia, 1997.
2. Vellas, B.; Wayne, S.; Romero, L.; Baumgartner, R.; Garry, P. Fear of falling and restriction of mobility in elderly fallers. *Age and Ageing* **1997**, *26*, 189–193.
3. Lord, S.; Sherrington, C.; Menz, H. *Falls in Older People: Risk Factors and Strategies for Prevention.*, 1st ed.; Cambridge University Press, 2001.
4. Delbaere, K.; Crombez, G.; Vanderstraeten, G.; Willems, T.; Cambier, D. Fear-related avoidance of activities, falls and physical frailty. A prospective community-based cohort study. *Age and Ageing* **2004**, *33*, 368–373.

5. Lord, S.; Ward, J.; Williams, P.; Anstey, K. An epidemiological study of falls in older community-dwelling women: the Randwick falls and fractures study. *Australian Journal of Public Health* **1993**, *17*, 240–245.
6. Henao, G.M.; Curcio Borrero, C.L.; Gómez Montes, J.F. Consecuencias De Las Caídas En Ancianos Institucionalizados. *Revista de la asociación Colombiana de Gerontología y Geriatría* **2009**, *23*, 1221–1233.
7. Igual, R.; Medrano, C.; Plaza, I. Challenges, issues and trends in fall detection systems. *BioMedical Engineering OnLine* **2013**, *12*, 1–24.
8. Shany, T.; Redmond, S.J.; Narayanan, M.R.; Lovell, N.H. Sensors-Based Wearable Systems for Monitoring of Human Movement and Falls. *IEEE Sensors Journal* **2012**, *12*, 658 – 670.
9. Pannurat, N.; Thiemjarus, S.; Nantajeewarawat, E. Automatic fall monitoring: A review. *Sensors* **2014**, *14*, 12900–12936.
10. Habib, M.A.; Mohktar, M.S.; Kamaruzzaman, S.B.; Lim, K.S.; Pin, T.M.; Ibrahim, F. Smartphone-Based Solutions for Fall Detection and Prevention: Challenges and Open Issues. *Sensors* **2014**, *14*, 7181–7208.
11. Sucerquia, A.; López, J.; Vargas-Bonilla, F. SisFall: A fall and movement dataset. *Sensors* **2017**, *17*, 1–14.
12. Igual, R.; Medrano, C.; Plaza, I. A comparison of public datasets for acceleration-based fall detection. *Medical Engineering and Physics* **2015**, *37*, 870–878.
13. Bagala, F.; Becker, C.; Cappello, A.; Chiari, L.; Aminian, K.; Hausdorff, J.M.; Zijlstra, W.; Klenk, J. Evaluation of Accelerometer-Based Fall Detection Algorithms on Real-World Falls. *Plos one* **2012**, *7*, e37062.
14. López, J.D.; Ocampo, C.; Sucerquia, A.; Vargas-Bonilla, F. Analyzing multiple accelerometer configurations to detect falls and motion. Latin American Congress on biomedical engineering, 2016.
15. Cola, G.; Avvenuti, M.; Vecchio, A.; Yang, G.Z.; Lo, B. An On-Node Processing Approach for Anomaly Detection in Gait. *IEEE Sensors Journal* **2015**, *15*, 6640 – 6649.
16. Oner, M.; Pulcifer-Stump, J.A.; Seeling, P.; Kaya, T. Towards the Run and Walk Activity Classification through Step Detection - An Android Application. 34th Annual International Conference of the IEEE EMBS, 2012, pp. 1980 – 1983.
17. Wundersitz, D.W.T.; Gastin, P.B.; Richter, C.; Robertson, S.J.; Netto, K.J. Validity of a trunk-mounted accelerometer to assess peak accelerations during walking, jogging and running. *European Journal of Sport Science* **2014**, *2014*, 382–390.
18. Clements, C.M.; Buller, M.J.; Welles, A.P.; Tharion, W.J. Real Time Gait Pattern Classification from Chest Worn Accelerometry During a Loaded Road March. 34th Annual International Conference of the IEEE EMBS, 2012.
19. López, J.D.; Sucerquia, A.; Duque-Muñoz, L.; Vargas-Bonilla, F. Walk and jog characterization using a triaxial accelerometer. IEEE International Conference on Ubiquitous Computing and Communications (IUCC), 2015, pp. 1406–1410.
20. Kalman, R.E. A New Approach to Linear Filtering and Prediction Problems. *Transactions of the ASME–Journal of Basic Engineering* **1960**, *82*, 35–45.
21. Bagalà, F.; Klenk, J.; Cappello, A.; Chiari, L.; Becker, C.; Lindemann, U. Quantitative Description of the Lie-to-Sit-to-Stand-to-Walk Transfer by a Single Body-Fixed Sensor. *IEEE Transactions on Neural Systems and Rehabilitation Engineering* **2013**, *21*, 624–633.
22. Berg, K.; Wood-Dauphinee, S.; Williams, J.; Maki, B. Measuring balance in the elderly: validation of an instrument. *Canadian Journal of Public Health* **1992**, *83*.
23. Otebolaku, A.M.; Andrade, M.T. User context recognition using smartphone sensors and classification models. *Journal of Network and Computer Applications* **2016**, *66*, 33–51.
24. Novak, D.; Rebersek, P.; De Rossi, S.M.M.; Donati, M.; Podobnika, J.; Beravs, T.; Lenzi, T.; Vitiello, N.; Carrozza, M.C.; Muniha, M. Automated detection of gait initiation and termination using wearable sensors. *Medical Engineering & Physics* **2013**, *35*, 1713–1720.
25. Yuan, X.; Yu, S.; Dan, Q.; Wang, G.; Liu, S. Fall Detection Analysis with Wearable MEMS-based Sensors. 16th International Conference on Electronic Packaging Technology (ICEPT), 2015, pp. 1184–1187.
26. Li, H.; li Yang, Y. Research of elderly fall detection based on dynamic time warping algorithm. Proceedings of the 35th Chinese Control Conference, 2016.
27. He, J.; Bai, S.; Wang, X. An Unobtrusive Fall Detection and Alerting System Based on Kalman Filter and Bayes Network Classifier. *Sensors* **2017**, *17*, 17.
28. Mao, A.; Ma, X.; He, Y.; Luo, J. Highly Portable, Sensor-Based System for Human Fall Monitoring. *Sensors* **2017**, *17*, 15.

29. Zhang, C.; Lai, C.F.; Lai, Y.H.; Wu, Z.W.; Chao, H.C. An inferential real-time falling posture reconstruction for Internet of healthcare things. *Journal of Network and Computer Applications* **2017**, *89*, 86–95.
30. Luenberger, D. An Introduction to Observers. *IEEE Transactions on Automatic Control* **1971**, *16(6)*, 596–602.
31. Noury, N.; Rumeau, P.; Bourke, A.; ÓLaighin, G.; Lundy, J. A proposal for the classification and evaluation of fall detectors. *IRBM* **2008**, *29*, 340–349.
32. Klenk, J.; Becker, C.; Lieken, F.; Nicolai, S.; Maetzler, W.; Alt, W.; Zijlstra, W.; Hausdorff, J.; van Lummel, R.; Chiari, L.; Lindemann, U. Comparison of acceleration signals of simulated and real-world backward falls. *Medical Engineering and Physics* **2011**, *33*, 368–373.
33. Noury, N.; Fleury, A.; Rumeau, P.; Bourke, A.; Laighin, G.; Rialle, V.; Lundy, J. Fall detection – Principles and Methods. 29th Annual International Conference of the IEEE EMBS, 2007, pp. 1663 – 1666.
34. Sisfall 2: Real-life/real-time elderly ADL. http://sistemic.udea.edu.co/en/research/projects/sucerquia2018/, 2018.